

Edgrewite $\text{Ca}_9(\text{SiO}_4)_4\text{F}_2$ -hydroxyledgrewite $\text{Ca}_9(\text{SiO}_4)_4(\text{OH})_2$, a new series of calcium humite-group minerals from altered xenoliths in the ignimbrite of Upper Chegem caldera, Northern Caucasus, Kabardino-Balkaria, Russia

EVGENY V. GALUSKIN,^{1,*} BILJANA LAZIC,² THOMAS ARMBRUSTER,² IRINA O. GALUSKINA,¹
NIKOLAI N. PERTSEV,³ VIKTOR M. GAZEEV,³ ROMAN WŁODYKA,¹ MATEUSZ DULSKI,⁴
PIOTR DZIERŻANOWSKI,⁵ ALEKSANDR E. ZADOV,⁶ AND LEONID S. DUBROVINSKY⁷

¹Faculty of Earth Sciences, Department of Geochemistry, Mineralogy and Petrography, University of Silesia, Będzińska 60, 41-200 Sosnowiec, Poland

²Mineralogical Crystallography, Institute of Geological Sciences, University of Bern, Freiestrasse 3, CH-3012 Bern, Switzerland

³Institute of Geology of Ore Deposits, Petrography, Mineralogy and Geochemistry (IGEM) RAS, Staromonetny 35, 119017 Moscow, Russia

⁴Institute of Physics, University of Silesia, Uniwersytecka 4, 40-007 Katowice, Poland

⁵Institute of Geochemistry, Mineralogy and Petrology, Warsaw University, al. Żwirki i Wigury 93, 02-089 Warszawa, Poland

⁶OOO Science Research Centre “NEOCHEM”, Dmitrovskoye Highway 100/2, 127238 Moscow, Russia

⁷Bayerisches Geoinstitut, Universität Bayreuth, D-95440 Bayreuth, Germany

ABSTRACT

Members of the edgrewite $\text{Ca}_9(\text{SiO}_4)_4\text{F}_2$ -hydroxyledgrewite $\text{Ca}_9(\text{SiO}_4)_4(\text{OH})_2$ series, structural analogues of clinohumite-hydroxylclinohumite series, $\text{Mg}_9(\text{SiO}_4)_4(\text{F},\text{OH})_2$, were discovered in xenoliths of carbonate-silicate rock altered to skarn within ignimbrites of the Upper Chegem volcanic structure, Kabardino-Balkaria, Northern Caucasus, Russia. The new minerals occur sparingly in zones containing bultfonteinite, hillebrandite, jennite, and chegemite, as well as rare relics of larnite and rondorfite enclosed in a matrix of hydroxyllestadite. Edgrewite and hydroxyledgrewite are largely altered to jennite in places with admixed zeophyllite and trabzonite, and are preserved as elongate relics mostly 0.1–0.4 mm long in the central part of atoll-like pseudomorphs. The new minerals form a solid-solution series $\text{Ca}_9(\text{SiO}_4)_4(\text{F},\text{OH})_2$, in which the content of the edgrewite end-member $\text{Ca}_9(\text{SiO}_4)_4\text{F}_2$ ranges from 74% (F = 3.64 wt%) to 31% (F = 1.52 wt%).

Structure refinement of crystals containing 51% and 37% of the edgrewite end-member gave, respectively, $R_1 = 3.03\%$, space group $P2_1/b11$ (no. 14), $Z = 2$, $a = 5.06870(10)$, $b = 11.35790(10)$, $c = 15.4004(2)$ Å, $\alpha = 100.5980(10)^\circ$, $V = 871.47(3)$ Å³; and $R_1 = 1.61\%$, space group $P2_1/b11$ (no. 14), $Z = 2$, $a = 5.06720(10)$, $b = 11.35450(10)$, $c = 15.3941(2)$ Å, $\alpha = 100.5870(10)^\circ$, and $V = 870.63(2)$ Å³.

Minerals of the edgrewite-hydroxyledgrewite series are colorless, optically biaxial (+), $2V_{\text{meas}} = 80(5)^\circ$; $2V_{\text{calc}} = 78.7^\circ$; dispersion $r > v$, medium; orientation: $Z = a$, $X \wedge c = 12(2)^\circ$; edgrewite: $\alpha = 1.621(2)$, $\beta = 1.625(2)$, $\gamma = 1.631(2)$; hydroxyledgrewite: $\alpha = 1.625(2)$, $\beta = 1.629(2)$, $\gamma = 1.635(2)$ (589 nm). The micro-hardness $\text{VHN}_{50} = 352\text{--}366$ kg/mm² corresponds to the Mohs scale of 5.5–6. FTIR spectra of edgrewite and hydroxyledgrewite show resolved bands at (edgrewite/hydroxyledgrewite, cm^{-1}): 3558 and 3551 and 3543/3554, absent/3486, 1075/1075, 996/996, 980/982, 934/933, 917/918, 904/903, 890/884, 864/864, 842/842, 818/820. Raman spectra are characterized by the following bands (edgrewite/hydroxyledgrewite, cm^{-1}) at: 921/923, 889/890, 839/840, and 815/814 (SiO_4 stretching), at: 556/559, 527/527, 423/419, 406/404, and 394/394 (SiO_4 bending), 309/295, 269/256, and 163/166 (CaO_6). In the OH stretching region three bands are noted at 3554, 3547, and 3540 cm^{-1} for edgrewite and two – 3550 and 3475 cm^{-1} for hydroxyledgrewite confirming the corresponding IR spectra. The major difference in Raman and IR spectra of edgrewite and hydroxyledgrewite is the presence of two resolved peaks in the OH stretching region at ca. 3550 and 3480 cm^{-1} for hydroxyledgrewite.

Keywords: New mineral, edgrewite, hydroxyledgrewite, humite, structure, Raman, FTIR, Russia

INTRODUCTION

Edgrewite $\text{Ca}_9(\text{SiO}_4)_4\text{F}_2$ and hydroxyledgrewite $\text{Ca}_9(\text{SiO}_4)_4(\text{OH})_2$, analogues of clinohumite $\text{Mg}_9(\text{SiO}_4)_4\text{F}_2$ and hydroxylclinohumite $\text{Mg}_9(\text{SiO}_4)_4(\text{OH})_2$, respectively, are two new Ca minerals of the humite group discovered in one of the seven large xenoliths (up to 20 m across, see geological map in Galuskin et al. 2009) of carbonate silicate skarn within the Upper Chegem caldera,

Northern Caucasus, Kabardino-Balkaria, Russia. The xenolith containing the two new minerals crops out on the slope of the small ridge joining Lakargi and Vorlan peaks at 3240 m above the sea level and 7 km from the Balkarian village Eltyubyu. Other Ca humite group minerals from the Upper Chegem caldera include kumtyubeite $\text{Ca}_5(\text{SiO}_4)_2\text{F}_2$ (Galuskina et al. 2009), chegemite $\text{Ca}_7(\text{SiO}_4)_3(\text{OH})_2$ (Galuskin et al. 2009), fluorchegemite $\text{Ca}_7(\text{SiO}_4)_3\text{F}_2$ (Galuskina et al. 2009, 2012), and reinhardbraunsite $\text{Ca}_5(\text{SiO}_4)_2(\text{OH})_2$, the type locality of which is

* E-mail: evgeny.galuskin@us.edu.pl

the Eifel district, Germany (Kirfel et al. 1983). In addition, these xenoliths are the type locality of a large number of new minerals, all discovered since 2007: garnet supergroup minerals: bitikleite $\text{Ca}_3\text{Sb}^{5+}\text{SnAl}_3\text{O}_{12}$ [originally named bitikleite-(SnAl)], usturite $\text{Ca}_3\text{Sb}^{5+}\text{ZrFe}_3^3\text{O}_{12}$ [originally named bitikleite-(ZrFe)], dzhuluite $\text{Ca}_3\text{Sb}^{5+}\text{SnFe}_3^3\text{O}_{12}$ [originally named bitikleite-(SnFe)], toturite $\text{Ca}_3\text{Sn}_2\text{Fe}_3^3\text{SiO}_{12}$, irinarassite $\text{Ca}_3\text{Sn}_2\text{Al}_2\text{SiO}_{12}$ and elbrusite $\text{Ca}_3\text{UZrFe}_3\text{O}_{12}$ [originally named elbrusite-(Zr)] (Galuskina et al. 2010a, 2010b, 2010c; 2011a, 2011b; Grew et al. 2012); perovskite group minerals: lakargiite CaZrO_3 , megawite CaSnO_3 (Galuskina et al. 2008, 2011a); calcio-olivine $\gamma\text{-Ca}_2\text{SiO}_4$ (Zadov et al. 2008); rusinovite $\text{Ca}_{10}(\text{Si}_2\text{O}_7)_3\text{Cl}_2$ (Galuskina et al. 2011b); pavlovskite $\text{Ca}_8(\text{SiO}_4)_2(\text{Si}_3\text{O}_{10})$ (Galuskina et al. 2012); vorlanite CaUO_4 (Galuskina et al. 2011c); eltybyuite $\text{Ca}_{12}\text{Fe}_{10}^{3+}\text{Si}_4\text{O}_{32}\text{Cl}_6$ (Galuskina et al. 2011d); magnesioeptunitite $\text{KNa}_2\text{LiMg}_2\text{Ti}_4^{3+}\text{Si}_8\text{O}_{24}$ (Zadov et al. 2011a) and aklimaite $\text{Ca}_4[\text{Si}_2\text{O}_5(\text{OH})_2](\text{OH})_4 \cdot 5\text{H}_2\text{O}$ (Zadov et al. 2011b).

Following Thompson (1978), a general formula for the calcium members of the humite-group can be written as $n\text{-Ca}_2\text{SiO}_4 + \text{Ca}_3(\text{SiO}_4)(\text{F,OH})_2$, where Ca_2SiO_4 represents the “calcio-olivine module” and $\text{Ca}_3(\text{SiO}_4)(\text{F,OH})_2$ the hypothetical “calcio-norbergitite module.” For $n = 1$, the formula leads to the kumtyubeite $\text{Ca}_5(\text{SiO}_4)_2\text{F}_2$ -reinhardbraunsite $\text{Ca}_5(\text{SiO}_4)_2(\text{OH})_2$ series ($\text{Ca}/\text{Si} = 5/2$ or $2.5/1$) isostructural with chondrodite; for $n = 2$, to the chegemite $\text{Ca}_7(\text{SiO}_4)_3(\text{OH})_2$ -fluorchegemite $\text{Ca}_7(\text{SiO}_4)_3\text{F}_2$ series ($\text{Ca}/\text{Si} = 7/3$ or $2.33/1$) isostructural with humite; for $n = 3$, to the edgrewite $\text{Ca}_9(\text{SiO}_4)_4\text{F}_2$ -hydroxyledgrewite $\text{Ca}_9(\text{SiO}_4)_4(\text{OH})_2$ series ($\text{Ca}/\text{Si} = 9/4$ or $2.25/1$) isostructural with clinohumite. Minerals with $\text{M}^{2+}/\text{Si} = 3/1$ ratio are absent in the polysomatic series of naturally occurring Ca- and Mn-humites, only the Mg-humite series has a 3/1 ratio-member: norbergite $\text{Mg}_3\text{SiO}_4(\text{F,OH})_2$ (Gibbs and Ribbe 1969; Ribbe 1982; Deer et al. 1982). However, the Mn analog of norbergite has been synthesized and its crystal structure refined (Zenser et al. 2000), whereas synthesis of a mixed Ca-Mg compound with norbergite stoichiometry, given as $\text{Ca}_2\text{SiO}_4\text{MgF}_2$, was reported by Christie (1965).

In the present paper, we describe the two new minerals edgrewite (IMA2011-58) and hydroxyledgrewite (IMA2011-113), approved by CNMNC IMA in September 2011 and March 2012, respectively. Edgrewite was named in honor of Edward S. Grew (b. 1944), a well-known scientist in the areas of mineralogy and petrology at the University of Maine. He also discovered or collaborated in the discovery of 10 new minerals, including boralsilite, khmaralite, stornesite-(Y), menzerite-(Y), and chopinite, as well as in the revalidation of prismatine. Since his first expedition to the Antarctic from 1972 to 1974 when he wintered at Molodezhnaya Station, Ed Grew has collaborated successfully with Russian scientists. Hydroxyledgrewite is a hydroxyl analog of edgrewite.

Type material is deposited in the collections of the Museum of Natural History, Bern, Switzerland, catalog numbers: NMBE 41086 (edgrewite) and in the Fersman Mineralogical Museum in Moscow, Russia, with the numbers: 4162/1 (edgrewite) and 4164/1 (hydroxyledgrewite).

METHODS OF INVESTIGATION

Investigations of morphology and composition of minerals were performed using a Philips XL30/EDAX scanning electron microscope (Department of Earth Sciences, University of Silesia, Poland) and CAMECA SX100 electron microprobes (WDS mode,

15 kV, 10–20 nA, 1–3 μm beam diameter; Institute of Geochemistry, Mineralogy and Petrology, University of Warsaw, Poland, and Electron Microscopy Laboratory, Polish Geological Institute, National Research Institute, Warsaw). The following lines, analytical crystals and standards were used for quantitative analyses of the edgrewite-hydroxyledgrewite series with the CAMECA SX100 electron microprobe: $\text{CaK}\alpha$, $\text{SiK}\alpha$ = wollastonite; $\text{FeK}\alpha$ = hematite; $\text{TiK}\alpha$ = rutile; $\text{MnK}\alpha$ = rhodonite; $\text{MgK}\alpha$ = diopside; $\text{NaK}\alpha$ = albite; $\text{AlK}\alpha$ = orthoclase; $\text{SK}\alpha$ = barite; $\text{FK}\alpha$ = fluorophlogopite.

Raman spectra of single crystals of edgrewite and hydroxyledgrewite were recorded using a Dilor XY spectrophotometer equipped with a 1800 line mm^{-1} grating monochromator, a charge-coupled device, Peltier-cooled detector and an Olympus BX40 confocal microscope (Bayerisches Geoinstitut, University of Bayreuth, Germany). The incident laser excitation was provided by a water-cooled argon laser source operating at 514.5 nm. The power at the exit of a $\times 100$ objective lens varied from 30 to 50 mW. Raman spectra were recorded in backscattering geometry in the range 100–4000 cm^{-1} and with a resolution of 2 cm^{-1} . Collection time was 20 s and 5 scans were obtained at each spot. The monochromator was calibrated using the Raman scattering line of a silicon plate (520.7 cm^{-1}).

Reflectance infrared spectra were measured using a Bio-Rad FTS-6000 spectrophotometer equipped with a Bio-Rad UMA-500 infrared microscope (Institute of Physics, University of Silesia, Poland). The 250×250 mm mercury cadmium telluride detector (MTC) in the microscope was cooled to 77 K using liquid nitrogen. Spectra were obtained in the range 6000–700 cm^{-1} with a resolution of 4 cm^{-1} . Interferograms were recorded by accumulating 512 scans and a gold-covered microscope slide was used to obtain the background spectrum. The reflection data were converted to standard absorption spectra using Fourier and Kramers-Krönig transformations.

Single-crystal X-ray studies on edgrewite [$\text{F}/(\text{OH} + \text{F}) = 0.51$] and hydroxyledgrewite [$\text{F}/(\text{OH} + \text{F}) = 0.37$] were carried out using a Bruker APEX II SMART diffractometer ($\text{MoK}\alpha$, $\lambda = 0.71073$ Å) in the Institute of Geological Sciences, University of Bern. Structural data on both minerals are consistent with monoclinic symmetry and systematic extinctions characteristic of space group: $P2_1/b11$, No. 14, $Z = 2$. Space group setting $P2_1/b11$ (α obtuse) is consistent with that determined by Taylor and West (1928) for clinohumite and is preferred over other settings because it permits direct comparison with minerals in the humite and olivine groups (Jones 1969).

Experimental details of both investigated crystals are summarized in Table 1. Single-crystal diffraction patterns showed that neither crystal was twinned. The diffraction pattern of what appeared to be the best crystal of edgrewite showed reflections due to admixed phases such as hillebrandite, bullfonteinite and a jennite-like mineral. Although these extraneous reflections were manually deducted, the poor R_{int} in Table 1 indicates that this pattern separation was only partly successful.

Diffraction data were collected with ω scans at different ϕ settings ($\phi\text{-}\omega$ scan) (Bruker 1999). Data were processed using SAINT (Bruker 1999). An empirical absorption correction using SADABS (Sheldrick 1996) was applied. The systematic absences were consistent with the space group $P2_1/b11$ (α obtuse) (No. 14). The structure of both crystals was solved by direct methods with subsequent analyses of difference-Fourier map and refined using neutral-atom scattering factors and the program SHELX97 (Sheldrick 2008). All fully occupied sites were refined with anisotropic displacement parameters. We used a split F9-O9 model where the atoms with shorter bonds to adjacent Ca were considered to be F9 and those forming the longer bonds were considered to be O9, representing an OH group (Galuskina et al. 2009). Both sites were constrained to a common isotropic displacement parameter and the sum of occupancies was fixed at 1. The split positions are separated by only ca. 0.26 Å. For hydroxyledgrewite the major H position (H1) was refined applying a distance restraint of 0.96(1) Å from the donor O9. A subordinate H site (H2) was extracted from the difference-Fourier map from a peak at 0.350, 0.059, 0.086, but the site was not refined. H⁺ has no electron and information on its position has to be extracted from the bonding electron between O and H. We justify the extraction in the case of hydroxyledgrewite as the peak can be interpreted as the bonding electron between O and H, and because a corresponding H site has been found in structural studies of related structures.

Collecting powder X-ray diffraction data, including a Gandolffi-like powder diffraction-pattern, which in principle is possible with a CCD equipped single-crystal diffractometer, was not attempted. A powder pattern collected with $\text{MoK}\alpha$ X-radiation is not useful for mineral identification using $\text{CuK}\alpha$ X-radiation because of differences in scattering factors and resulting intensities. Moreover, the presence of admixed phases would complicate interpretation of the patterns. Consequently, the X-ray powder patterns (Tables 2 and 3; supplementary materials¹ for $\text{CuK}\alpha$

¹ Deposit item AM-12-096, Figures 1 and 7; Tables 2, 3, 5, 6, 8, 9, and 10. Deposit items are available two ways: For a paper copy contact the Business Office of the Mineralogical Society of America (see inside front cover of recent issue) for price information. For an electronic copy visit the MSA web site at <http://www.minsocam.org>, go to the *American Mineralogist* Contents, find the table of contents for the specific volume/issue wanted, and then click on the deposit link there.

TABLE 1. Parameters for X-ray data collection and crystal-structure refinement for edgrewite and hydroxyledegrewite

	Edgrewite	Hydroxyledegrewite
Cell dimensions (Å)	$a = 5.06870(10)$ $b = 11.35790(10)$ $c = 15.4004(2)$ $\alpha = 100.5980(10)^\circ$ $\beta = 90.00^\circ$ $\gamma = 90.00^\circ$	$a = 5.06720(10)$ $b = 11.35450(10)$ $c = 15.3941(2)$ $\alpha = 100.5870(10)^\circ$ $\beta = 90.00^\circ$ $\gamma = 90.00^\circ$
Cell volume (Å ³)	871.47(2)	870.63(2)
Space group	$P2_1/b11$ (No. 14)	$P2_1/b11$ (No. 14)
Z	2	2
Chemical formula	$\text{Ca}_9(\text{SiO}_4)_4(\text{F,OH})_2$	$\text{Ca}_9(\text{SiO}_4)_4(\text{OH,F})_2$
Note	H site not refined	H site refined
Diffractometer	Bruker APEX II	Bruker APEX II
X-ray radiation	MoK α (0.71073 Å)	MoK α (0.71073 Å)
X-ray power	50 kV, 35 mA	50 kV, 35 mA
Temperature	293 K	293 K
Crystal size (mm)	0.14 × 0.12 × 0.05	0.12 × 0.12 × 0.40
Time per frame	120 s	30 s
Number of frames	1800	1314
Completeness	99.8%	99.9%
Average redundancy	4.983	3.738
Reflections collected	13206	9902
Max. θ	30.51	30.51
Index range	$-7 \leq h \leq 7$ $-21 \leq l \leq 22$ $-16 \leq k \leq 13$	$-16 \leq k \leq 15$ $-7 \leq h \leq 7$ $-19 \leq l \leq 21$
Unique reflections	2650	2694
Reflections > $2\sigma(I)$	2008	2378
Number of parameters	142	146
R_{int}	0.0991	0.0208
R_σ	0.0634	0.0178
Goof	0.930	1.055
$R1, I > 2\sigma(I)$	0.0303	0.0161
$R1, \text{all data}$	0.0409	0.0189
wR2 (on F^2)	0.0720	0.0454
$\Delta\rho_{\text{min}}$ ($-\text{e}\cdot\text{Å}^{-3}$)	-0.569 close to Si2	-0.31 close to Si2
$\Delta\rho_{\text{max}}$ ($\text{e}\cdot\text{Å}^{-3}$)	0.792 close to Ca5	0.42 close to H

1.540598 Å) were calculated from the refined coordinates of the crystal-structures using the program PowderCell for Windows version 2.4 (Kraus and Nolze 1996). A powder pattern can be calculated for any diffraction symmetry and wavelength with PowderCell.

OCCURRENCE AND ORIGIN

Edgrewite and hydroxyledegrewite, were discovered in xenolith no. 1, which is the largest of 7 xenoliths (xenolith numbering after Gazeev et al. 2006 and Galuskin et al. 2009) in ignimbrites of the Upper Chegem caldera. Samples with minerals of the edgrewite-hydroxyledegrewite series were collected in 2009, during mineralogical mapping of the xenolith no. 1, at 1.5 m from the eastern contact of the xenolith with unaltered ignimbrite. This part of xenolith no. 1 appears to be a fragment in a contact breccia comprising altered sedimentary fragments and ignimbrite material. It is the only xenolith in which a core (~2 m) composed of periclase (brucite) marble is preserved. The brucite marble is surrounded by the following successive zones from core to contact with ignimbrite: spurrite, kumtyubeite-reinhardbraunsite, chegemite, and larnite (Galuskin et al. 2009). In the immediate contact with unaltered ignimbrite thin successive zones a few millimeters wide are noted: wollastonite $\text{CaSiO}_3 \rightarrow$ rankinite $\text{Ca}_3\text{Si}_2\text{O}_7 \rightarrow$ pavlovskyite $\text{Ca}_8(\text{SiO}_4)_2(\text{Si}_3\text{O}_{10})$ (Galuskin et al. 2012). The proportion of fluorine-bearing silicates tends to increase toward the contact with ignimbrite (Galuskin et al. 2009). Edgrewite is confined to the fragments of rocks enriched with fluorine (with abundant fluorchegemite and secondary bultfonteinite) (Fig. 1B, supplementary materials¹).

Bultfonteinite, hillebrandite, jennite, and chegemite-fluorchegemite are the most widespread minerals associated with edgrewite and hydroxyledegrewite. Relics of high-temperature larnite skarn are preserved within yellow patches. Minerals of the ettringite group, hydrocalumite, awfillite, and “hydrogarnet,” which are characteristic of most skarns in the Upper Chegem caldera, are less common in the skarn containing edgrewite and hydroxyledegrewite.

Edgrewite was found sparingly in cream-colored fragments about 2–3 cm in size of strongly altered skarn (Figs. 1A–1B, supplementary materials¹), whereas hydroxyledegrewite was found sparingly in a sample collected in the same profile 10 cm toward the center from the edgrewite sample. To the naked eye, the samples with edgrewite and hydroxyledegrewite are very similar in appearance. Edgrewite and hydroxyledegrewite are largely altered to jennite, in places with admixed zeophyllite and trabzonite, and are preserved as elongate relics mostly 0.1–0.4 mm long in the central part of atoll-like pseudomorphs, which are mantled by a thin outer rim of fluorine-bearing hillebrandite and bultfonteinite (Fig. 1B, supplementary materials¹; Fig. 2). The atoll-like pseudomorphs generally do not exceed few hundred micrometers (Fig. 2A), a few hydroxyledegrewite pseudomorphs are up to 1 mm long (Figs. 2B–2C).

The xenoliths are interpreted to be terrigenous-carbonate rocks metamorphosed to calc-silicate skarn under conditions of the sanidinite facies ($T > 900^\circ\text{C}$ and $P < 1\text{--}2$ kbar; Zharikov et al. 1998; Galuskin et al. 2009, 2012). Edgrewite and hydroxyledegrewite formed at somewhat lower temperatures during retrogression following crystallization of the larnite skarns. The successive formation of Ca-humites from altered primary silicates and minerals of the ellestadite series in larnite skarns is accompanied by an increase of the Si:Ca ratio in humite minerals from edgrewite-hydroxyledegrewite (Ca/Si = 2.25/1) to chegemite-fluorchegemite (Ca/Si = 2.33/1) and kumtyubeite-reinhardbraunsite (Ca/Si = 2.5/1). The more fluorine rich humite-group minerals crystallize at the beginning of this process, followed by more OH-rich humite minerals (Galuskina et al. 2009). It cannot be ruled out that more fluorine-rich edgrewite can crystallize together with larnite, but such crystals were not detected as relics in the primary ellestadite skarns (Fig. 1C, supplementary materials¹). Probably, in xenolith no.1 edgrewite (Ca/Si = 2.25/1) crystallized in fragments of larnite (Ca/Si = 2/1) skarns enriched with galuskinite $\text{Ca}_7(\text{SiO}_4)_3\text{CO}_3$ (Ca/Si = 2.33/1). Our preliminary investigations on zones with chegemite $\text{Ca}_7(\text{SiO}_4)_3(\text{OH,F})_2$ from xenolith no.7 show that they form from alteration of galuskinite-larnite skarns. Galuskinite is a new mineral, recently described from calcium high-temperature skarn of the Birkhin Massif (Baikal, Russia) (Lazic et al. 2011).

PHYSICAL AND OPTICAL PROPERTIES

Minerals of the edgrewite-hydroxyledegrewite series exhibit similar physical properties. They are colorless, transparent in small grains and thin section, and possess a pronounced vitreous lustre. These minerals are white in aggregates and give a white streak. Rare crystals of edgrewite-hydroxyledegrewite (point symmetry $2/m$) show combinations of pinacoids $\{010\}$, $\{100\}$, $\{001\}$ and rhombic prisms $\{110\}$, $\{011\}$, $\{101\}$ as inferred from faces observed on crystals in thin section. Simple and polysynthetic

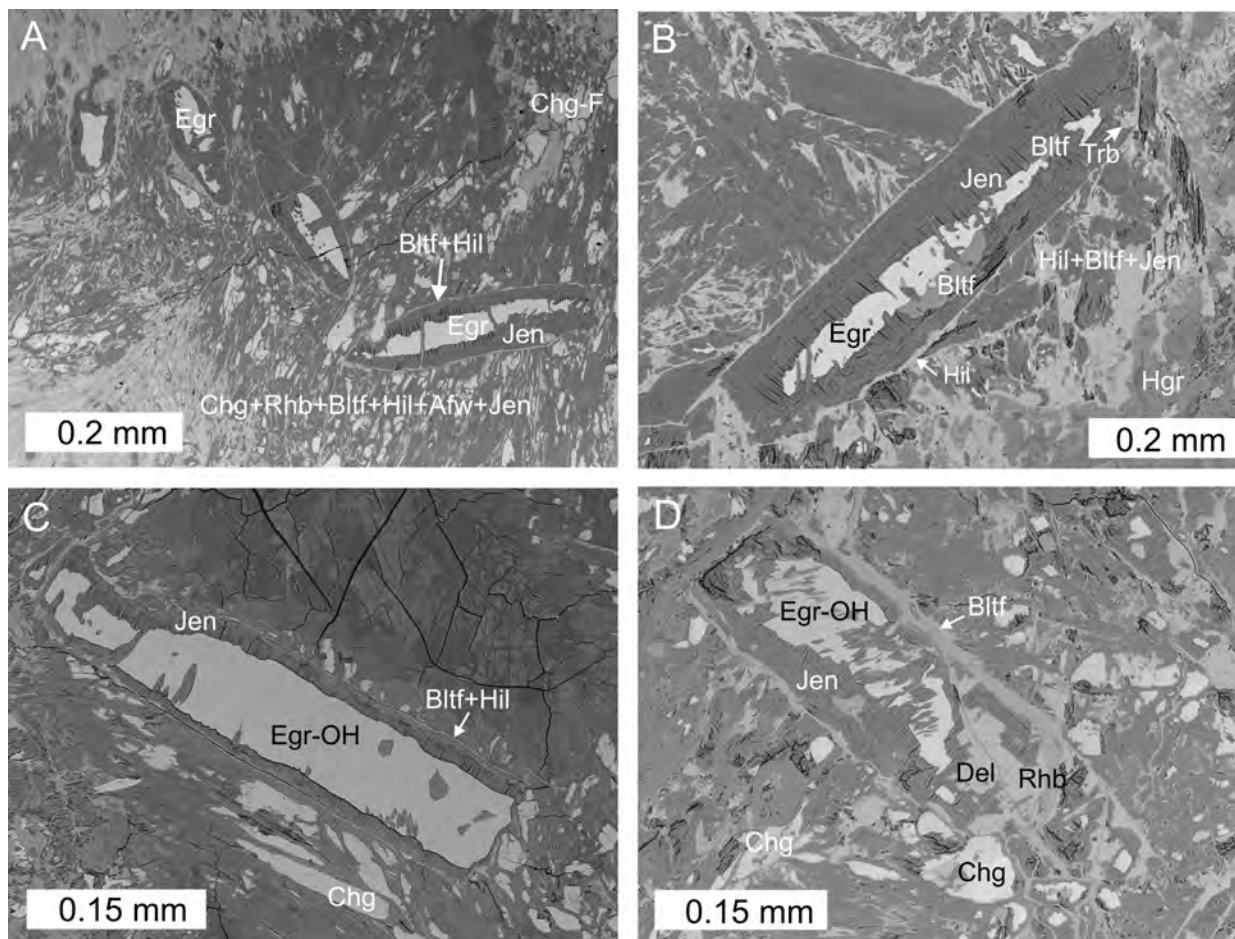


FIGURE 2. Backscattered electron images of minerals of edgrewite-hydroxyledgrewite series in altered skarn. (A) Lenticular, atoll-like microstructure resulting from partial replacement of edgrewite by jennite; (B) partial replacement of edgrewite by jennite and subordinate bultfonteinite, which is surrounded by thin mantle of hillebrandite; (C) the largest hydroxyledgrewite crystal, which was used for structure refinement, Raman spectroscopy, and optical studies; (D) hydroxyledgrewite relics in atoll-like pseudomorph associated with reinhardbraunsite and chegemite. Afw = awillite, Bltf = bultfonteinite, Chg = chegemite-fluorchegemite, Del = dellaite, Egr = edgrewite, Egr-OH = hydroxyledgrewite, Ell = hydroxyllellstadite, Jen = jennite, Lar = larnite, Hil = hillebrandite, Rhb = reinhardbraunsite, Trb = trabzonite.

twins on (010) are present. The (010) cleavage is good. The micro-hardness $VHN_{50} = 366 \text{ kg/mm}^2$ for edgrewite (mean of 3) and $VHN_{50} = 352366 \text{ kg/mm}^2$ for hydroxyledgrewite (mean of 4) correspond to 5.5–6 on the Mohs scale.

Edgrewite (Table 4, analysis 3) and hydroxyledgrewite (Table 4, analysis 6) are biaxial (+) and have the following optical properties: $\alpha = 1.621(2)$, $\beta = 1.625(2)$, $\gamma = 1.631(2)$, $\delta = 0.010$ (589 nm) and $\alpha = 1.625(2)$, $\beta = 1.629(2)$, $\gamma = 1.635(2)$, $\delta = 0.010$ (589 nm), respectively. The other optical characteristics are similar for both minerals: $2V(\text{meas}) = 80(5)^\circ$, $2V(\text{calc}) = 78.7^\circ$; dispersion medium, $r > v$; $Z = a$, $X \wedge c = 12(2)^\circ$. Density could not be measured because of small grain size; calculated density (g/cm^3) = 2.918 (Table 4, analysis 1, edgrewite), 2.920 (Table 4, analysis 2, edgrewite), 2.921 (Table 4, analysis 3, edgrewite), 2.920 g/cm^3 (Table 4, analysis 5, hydroxyledgrewite), 2.916 g/cm^3 (Table 4, analysis 6, hydroxyledgrewite).

Gladstone-Dale's compatibility factors $[1 - (K_p/K_c)] =$

-0.035 (excellent for analysis 3, Table 4, edgrewite) and -0.036 (excellent for analysis 6, Table 4, hydroxyledgrewite), using the appropriate empirical formulas.

CHEMICAL COMPOSITION

Edgrewite and hydroxyledgrewite form a solid-solution $\text{Ca}_9(\text{SiO}_4)_4(\text{F},\text{OH})_2$ (Table 4), in which the proportion of the edgrewite (Egr) end-member $\text{Ca}_9(\text{SiO}_4)_4\text{F}_2$ ranges from 31% at F = 1.52 wt% (analysis 7) to 74% at F content = 3.64 wt% (analysis 4). Electron microprobe analyses gave $\text{F}/(\text{F}+\text{OH}) = 0.51$ and 0.37, respectively, for the edgrewite and hydroxyledgrewite crystals used for structure refinement. These anion compositions are in good agreement with anion composition determined from refined F occupancy at the O9 site, $\text{F}/(\text{F}+\text{OH}) = 0.52$ and 0.39, respectively (see below). There is continuous solid solution between $\text{Egr}_{38}\text{-Egr}_{74}$ (Fig. 3). No other constituents, i.e., Ti, Fe, and Mn, are present in amounts exceeding 0.1 wt% oxide.

TABLE 4. Chemical composition of minerals in the edgrewite-hydroxyledegrewite series

	1		2		3		4		5		6		7				
	S.D.	range	S.D.	range	S.D.	range	S.D.	range	S.D.	range	S.D.	range	S.D.	range			
Wt%																	
SiO ₂	31.19	0.32	30.43–31.53	31.46	0.15	31.27–31.66	30.90	0.18	30.61–31.30	31.10	31.29	0.35	30.84–31.71	31.07	0.11	30.82–31.26	31.10
TiO ₂	0.08	0.03	0.04–0.13	n.d.			0.06	0.04	0–0.15	n.d.	0.06	0.03	0.02–0.10	0.07	0.02	0.02–0.10	n.d.
CaO	65.70	0.28	65.28–66.07	66.43	0.30	66.10–66.91	65.70	0.33	65.03–66.21	65.27	65.99	0.28	65.12–66.71	65.34	0.25	64.70–65.78	65.33
FeO	0.02	0.02	0–0.13	0.08	0.06	0.03–0.17	0.03	0.04	0–0.12	n.d.	0.07	0.06	0–0.16	n.d.			n.d.
MnO	0.03	0.03	0–0.08	0.06	0.05	0–0.12	0.04	0.04	0–0.13	n.d.	0.05	0.05	0–0.17	n.d.			n.d.
F	3.03	0.25	2.77–3.64	2.87	0.31	2.48–3.52	2.52	0.12	2.42–3.11	3.64	2.09	0.15	1.88–2.27	1.82	0.16	1.52–2.13	1.52
H ₂ O*	0.91			1.01			1.01			0.60	1.36			1.47			1.61
–O=F	1.29			1.22			1.07			1.53	0.88			0.76			0.65
Total	99.67			100.69			99.33			100.61	100.03			99.00			98.91
Formulas																	
Ca	9.000			9.006			9.025			8.998	9.000			8.999			9.001
Fe ²⁺	0.002			0.008			0.003				0.006						
Mn ²⁺	0.003			0.006			0.005				0.005						
Si	3.988			3.980			3.962			4.002	3.983			3.994			3.999
Ti ⁴⁺	0.008						0.006				0.006			0.006			
F	1.226			1.148			1.024			1.481	0.843			0.738			0.62
OH	0.774			0.852			0.977			0.518	1.156			1.261			1.38
Egr	61			57			51			74	42			37			31
Egr-OH	39			43			49			26	58			63			69

Notes: 1 = central parts of edgrewite grains in Figure 2A, mean of 13; 2 = edgrewite grains shown in Figure 2B, mean of 9; 3 = edgrewite crystal was used for single-crystal XRD and Raman study, mean of 21; 4 = edgrewite analysis with maximum fluorine content, 5 = hydroxyledegrewite grain with chegemite, mean of 9, Figure 2D; 6 = hydroxyledegrewite crystal was used for single-crystal XRD and Raman study, mean of 29, Figure 2C; 7 = hydroxyledegrewite analysis with minimum fluorine content. Egr = edgrewite; Egr-OH = hydroxyledegrewite. Formula calculated on 13 cations and 18(O+F+OH).

* Calculated on charge balance.

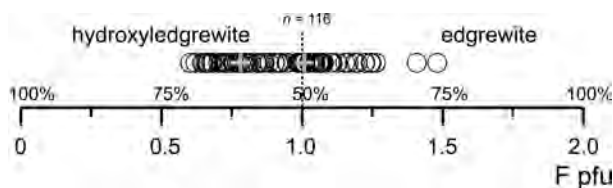


FIGURE 3. Plot of F/(F+OH) ratios in minerals of the edgrewite-hydroxyledegrewite series, showing the division between the two species. The percentages indicate the proportion of the Ca₉(SiO₄)₄F₂ end-member. Crosses = compositions of grains used for single-crystal analysis.

INFRARED AND RAMAN SPECTROSCOPY

Infrared and Raman spectra of edgrewite and hydroxyledegrewite are similar and show major differences only in the region of OH vibrations (Fig. 4 and 5). Reflectance FTIR spectra of edgrewite and hydroxyledegrewite (1100–800 cm⁻¹ region) converted to a standard absorption spectrum using Fourier and Kramers-Krönig transformations correspond to the various stretching vibrations of SiO₄ tetrahedra yielding the following main bands (edgrewite/hydroxyledegrewite, cm⁻¹): 1075/1075, 996/996, 980/982, 934/933, 917/918, 904/903, 890/884, 864/864, 842/842, 818/820 (Figs. 4A and 4B). Similarly as for the humite group minerals the main SiO₄ stretching modes are centered near 900 cm⁻¹ (Frost et al. 2007a, 2007b). The 3600–3400 cm⁻¹ region relating to OH stretching vibrations displays one complex band in spectrum of edgrewite, which consists of the three overlapping bands at 3558, 3551, and 3543 cm⁻¹ (Fig. 4C), whereas the hydroxyledegrewite spectrum shows a single strong band at 3554 cm⁻¹ and an additional band at 3486 cm⁻¹ (Fig. 4D).

The Raman spectra of edgrewite and hydroxyledegrewite are shown in Figure 5. In the 750 to 1000 cm⁻¹ region there is a characteristic pattern of four bands (edgrewite/hydroxyledegrewite, cm⁻¹): 921/923, 889/890, 839/840, and 815/814 related to stretching vibrations of SiO₄. In the 350 to 750 cm⁻¹ region

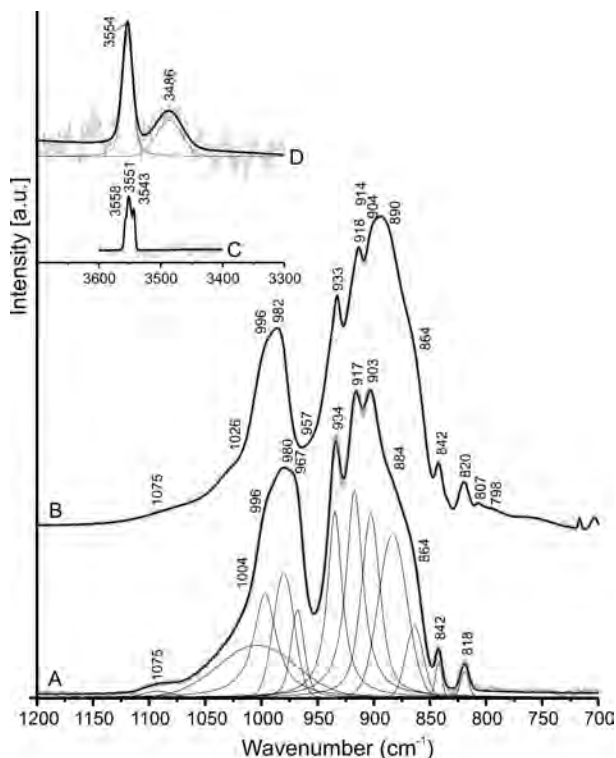


FIGURE 4. FTIR spectra of edgrewite (A and C) and hydroxyledegrewite (B and D).

corresponding to the bending vibrations of the SiO₄ units following bands are found (edgrewite/hydroxyledegrewite, cm⁻¹): 556/559, 527/527, 423/419, 406/404, and 394/394. Bands in the region below 350 cm⁻¹ correspond mainly to vibrations of the CaO₆ octahedra.

In the OH stretching region one complex band near 3550

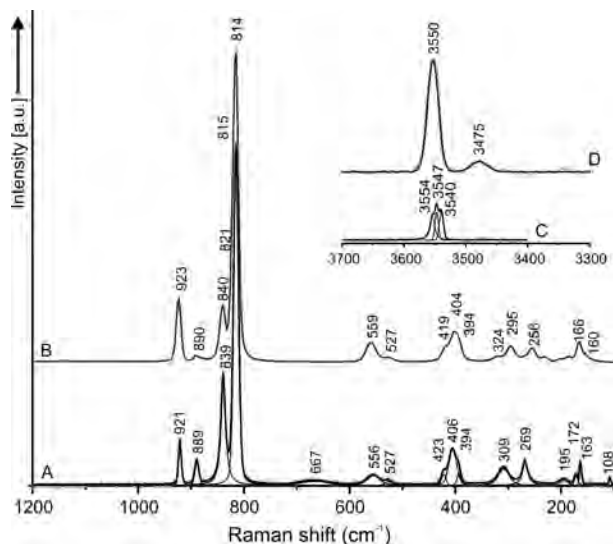


FIGURE 5. Raman spectra of edgrewite (A and C) and hydroxyledgrewite (B and D).

cm^{-1} in the edgrewite spectrum and two bands at 3475 and 3550 cm^{-1} in the hydroxyledgrewite spectrum correspond to bands in the IR spectra (Figs. 5C and 5D). FTIR and Raman spectra of edgrewite in the region of OH groups are very similar to those of kumtyubeite $\text{Ca}_3(\text{SiO}_4)_2\text{F}_2$ (Galuskina et al. 2009), and spectra of hydroxyledgrewite are similar to reinhardbraunsite (Galuskina et al. 2009) and chegemite (Galuskin et al. 2009).

DISTINGUISHING THE CALCIUM HUMITE-GROUP MINERALS

Optical microscopy can be applied to distinguishing the Ca humite-group minerals. Minerals of the kumtyubeite-reinhardbraunsite series have smaller $2V$ and slightly lower refraction indices in comparison with minerals of the chegemite and edgrewite series (Table 5, supplementary materials¹). Kumtyubeite-reinhardbraunsite and chegemite-fluorchegemite are optically negative; only edgrewite and hydroxyledgrewite are positive. Parallel extinction distinguishes chegemite from monoclinic Ca-humite minerals. Comparison of EMPA data of Ca-humite minerals with different Ca/Si ratio obtained at the same measurement session shows that problems can occur only in distinguishing chegemite-fluorchegemite from edgrewite-hydroxyledgrewite, which have similar wt% contents of CaO and SiO_2 (Table 6, supplementary materials¹). Fluorine and hydroxyl Ca-humite minerals are readily distinguished by Raman or FTIR spectroscopy in the OH region: two bands near 3550–3560 and 3475–3480 cm^{-1} are observed on OH-dominant Ca-humite spectra (chegemite, reinhardbraunsite, hydroxyledgrewite), whereas only one band near 3550 cm^{-1} is observed on F-dominant Ca-humite spectra (kumtyubeite, fluorchegemite, edgrewite) (Figs. 4 and 5; Galuskina et al. 2009; Galuskin et al. 2009).

CRYSTAL STRUCTURE OF EDGREWITE AND HYDROXYLEDGREWITE AND H-BONDING

The crystal structure of edgrewite and hydroxyledgrewite (Fig. 6, Tables 1 and 7a, 7b; and supplementary materials¹: Tables

8a, 8b, 9, and 10) corresponds to the clinohumite structure-type (e.g., Robinson et al. 1973; Ferraris et al. 2000; Friedrich et al. 2001; Berry and James 2001). A projection of a polyhedral structure model of edgrewite along [100] (Fig. 6) is indistinguishable from a corresponding diagram for clinohumite. Figure 7 (supplementary materials¹) illustrates the obvious difference between the structures due to the increase in anion-anion distance. The cell volume of edgrewite is ca. 24% greater than that of clinohumite end-member due to the difference in octahedral ionic radii, 0.72 Å for Mg vs. 1.00 Å for Ca (Shannon 1976). Thus, the mean octahedral Ca-O distances in edgrewite are 2.36 Å compared to Mg-O = 2.11 Å in clinohumite. Minerals of the humite group have hexagonal closest packing of anions, which is characteristic of minerals related to olivine, but with increasing radius of the cation at the octahedral sites, the closest anion packing increasingly deviates from an “ideal” closest packing (Fig. 7, supplementary materials¹). This deviation is characteristic of calcio-olivine (Smith et al. 1965; Czaya 1971; Udagawa et al. 1980; Mumme et al. 1995; Gobechiya et al. 2008; Yamnova et al. 2011) and other Ca humite-group minerals (Kirfel et al. 1983; Galuskina et al. 2009, 2012; Galuskin et al. 2009). Because the relatively rigid SiO_4 tetrahedra share three edges with the large CaO_6 octahedra, there are large angular distortions of the O-Ca-O angles.

Hydrogen bonds in hydroxyledgrewite (Fig. 8) are associated with O9, F9, and O8, and show positional disorder, a feature

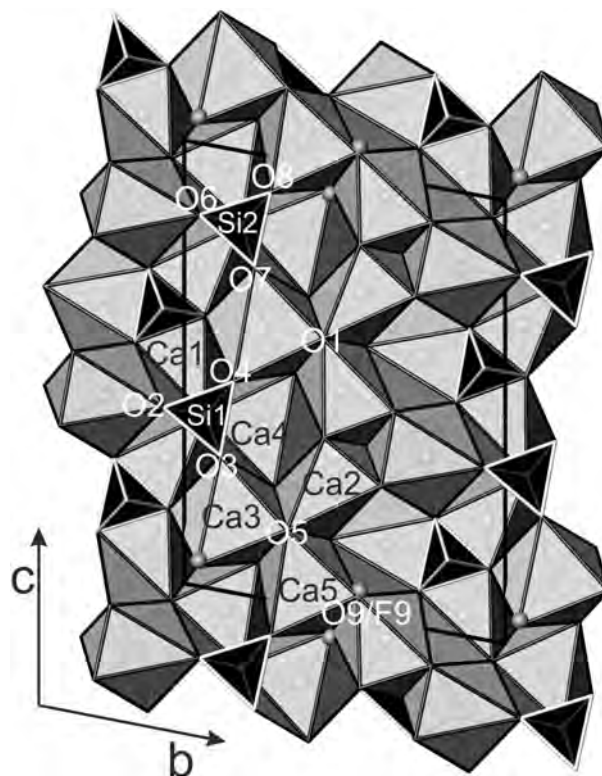


FIGURE 6. Polyhedral drawing of the edgrewite structure projected along *a* in $P2_1/c11$ setting. Small gray spheres at octahedral corners represent F9/O9 sites. SiO_4 groups are black with white rims, CaO_6 octahedra are gray with black rims.

TABLE 7a. Atomic coordinates and equivalent isotropic atomic displacement parameters (\AA^2) for edgrewite

Atom	Occ	x	y	z	$U_{\text{eq}}/U_{\text{iso}}$
Ca1	1	0.5	0.0	0.5	0.00692(12)
Ca2	1	0.49508(8)	0.94666(4)	0.27370(3)	0.00698(10)
Ca3	1	0.00478(8)	0.13653(4)	0.17283(3)	0.00645(10)
Ca4	1	0.50769(8)	0.25407(4)	0.38901(3)	0.00606(10)
Ca5	1	0.49245(8)	0.87168(4)	0.04256(3)	0.00696(10)
Si1	1	0.07123(11)	0.06835(5)	0.38955(4)	0.00430(12)
Si2	1	0.07549(11)	0.17901(5)	0.83411(4)	0.00466(13)
O1	1	0.7511(3)	0.06609(13)	0.38803(10)	0.0074(3)
O2	1	0.2986(3)	0.43501(13)	0.38809(10)	0.0062(3)
O3	1	0.2028(3)	0.11311(13)	0.30359(10)	0.0070(3)
O4	1	0.2017(3)	0.15466(13)	0.47638(10)	0.0073(3)
O5	1	0.2550(3)	0.32030(13)	0.16362(10)	0.0075(3)
O6	1	0.7950(3)	0.95261(12)	0.16185(10)	0.0068(3)
O7	1	0.7041(3)	0.28081(13)	0.25414(10)	0.0073(3)
O8	1	0.7073(3)	0.23059(13)	0.08118(10)	0.0067(3)
O9	0.52(2)	0.2285(12)	0.0404(4)	0.0445(5)	0.0092(5)*
F9	0.48(2)	0.2619(11)	0.0459(4)	0.0585(4)	0.0092(5)*

Note: U_{eq} is defined as one third of the trace of the orthogonalized U_{ij} tensor.
* Isotropic displacement parameters (U_{iso}) were constrained to be equal for O9 and F9.

TABLE 7b. Atomic coordinates and equivalent isotropic atomic displacement parameters (\AA^2) for hydroxyledegrewite

Atom	Occ	x	y	z	$U_{\text{eq}}/U_{\text{iso}}$
Ca1	1	0.5	0.0	0.5	0.00884(7)
Ca2	1	0.49509(4)	0.946623(18)	0.273691(14)	0.00896(6)
Ca3	1	0.00492(4)	0.136528(19)	0.172791(14)	0.00835(6)
Ca4	1	0.50779(4)	0.254077(19)	0.388989(14)	0.00798(6)
Ca5	1	0.49252(4)	0.871677(19)	0.042505(15)	0.00889(6)
Si1	1	0.07117(6)	0.06837(2)	0.389501(18)	0.00639(7)
Si2	1	0.07545(6)	0.17905(2)	0.83406(19)	0.00666(7)
O1	1	0.75075(15)	0.06615(6)	0.38795(5)	0.00930(15)
O2	1	0.29857(15)	0.43467(6)	0.38816(5)	0.00824(14)
O3	1	0.20261(15)	0.11343(6)	0.30367(5)	0.00882(15)
O4	1	0.20156(15)	0.15466(6)	0.47629(5)	0.00917(15)
O5	1	0.25522(15)	0.32029(6)	0.16366(5)	0.00967(15)
O6	1	0.79505(15)	0.95277(6)	0.16192(5)	0.00910(15)
O7	1	0.70380(15)	0.28052(6)	0.25421(5)	0.00910(15)
O8	1	0.70743(15)	0.23048(6)	0.08132(5)	0.00904(15)
O9	0.608(12)	0.2309(6)	0.04123(18)	0.0463(2)	0.0100(2)*
F9	0.392(12)	0.2672(7)	0.0464(2)	0.0594(3)	0.0100(2)*
H1	0.6	0.091(11)	-0.012(5)	0.023(5)	0.023(3)

Note: U_{eq} is defined as one third of the trace of the orthogonalized U_{ij} tensor.
* Isotropic displacement parameters (U_{iso}) were constrained to be equal for O9 and F9.

characteristic of the humite group (e.g., Friedrich et al. 2001; Berry and James 2001; Galuskina et al. 2009; Galuskin et al. 2009). O9 sites are related by the inversion center at the origin, and are separated by 2.81 \AA in hydroxyledegrewite and 2.76 \AA in edgrewite (Table 9, supplementary materials) vs. 2.89 \AA in hydroxylclinohumite (Berry and James 2001). O9 is coordinated to Ca3 and 2 \times Ca5, and acts both as donor and acceptor of a hydrogen bond (Fig. 8A). In edgrewite the proton (H1) is positioned close to the inversion center (Fig. 8A) and the hydrogen bond is accepted by the opposite F9: O9-H1 \cdots F9, $D_{\text{O-F}} = 3.01 \text{\AA}$, i.e., the hydrogen bond O9-H1 protrudes out of the plane formed by Ca3 and 2 \times Ca5.

In hydroxyledegrewite, there are two different hydrogen bonds similar to those reported in hydroxylclinohumite (Berry and James 2001), one of which has already been described above: O9-H1 \cdots F9, $D_{\text{O-F}} = 3.07 \text{\AA}$ or O9-H1 \cdots O9, $D_{\text{O-O}} = 2.81 \text{\AA}$. To avoid short H \cdots H distances, the second hydrogen bond O9-H2 \cdots O8 also protrudes out of the triangular plane but nearly in the opposite direction (Fig. 8B). In hydroxyledegrewite the O9 \cdots O8 distance is 3.21 \AA , whereas the corresponding distance in hydroxylclinohumite is 2.85 \AA (Berry and James 2001).

The ionic radius of three-coordinated F is 1.30 \AA , slightly less than the 1.34 \AA for three-coordinated O belonging to an OH group (Shannon 1976). Thus, in minerals containing both F and OH and isostructural with clinohumite, the position F9 is almost at the center of the triangle formed by Ca3 and 2 \times Ca5, whereas O9 lies outside the plane to accommodate the longer Ca-O distances. If the hydrogen bond O9-H1 \cdots O9 or O9-H1 \cdots F9 is active, then the donor O9 is displaced from the plane toward the center of symmetry (Fig. 8A). However, what is the direction of O9 displacement if the opposite pointing hydrogen bond O9-H2 \cdots O8 is active? In case of hydroxyledegrewite the potential hydrogen position H2 is 0.86 \AA from O9, but too close (2.2–2.4 \AA) to the Ca sites constituting the triangle. If O9 were displaced to the opposite side of the triangle to enable physically meaningful Ca H2 separation, then the split position model (F9, O9) to determine the degree of F9 for O9 substitution is not correct. The real model would require splitting into three sites (O9, F9, and O9), which cannot be realized in the refinement procedure

because of the very short distances between these sites, 0.27 \AA . The O9 splitting problem also remains unresolved even after the powder neutron-diffraction study of deuterated synthetic hydroxylclinohumite (Berry and James 2001). Our calculation of D2 \cdots Mg distances from the positions reported by Berry and James (2001) gave 2.15 \AA , which is in the same range as O-Mg bonds (Mg3-O varies between 2.05 and 2.19 \AA) and thus too short. Smearing due to positional disorder cannot be analyzed because Berry and James (2001) refined all sites with an isotropic displacement model.

OH-specific Raman/FTIR frequencies around 3500 cm^{-1} are very similar, at 3561/3558, 3553/3551, and 3544/3541 cm^{-1} for kumtyubeite $\text{Ca}_5(\text{SiO}_4)_2(\text{F,OH})_2$ (Galuskina et al. 2009), and at 3554/3558, 3547/3551 and 3540/3543 cm^{-1} for edgrewite $\text{Ca}_9(\text{SiO}_4)_4(\text{F,OH})_2$ (Figs. 4C–4D and 5C–5D). Appearance of an additional band near 3480 cm^{-1} is the principal distinction between OH-dominant and F-dominant humite-group minerals. For example, in the Raman spectra of reinhardbraunsite $\text{Ca}_5(\text{SiO}_4)_2(\text{OH,F})_2$ there are a doublet 3562 and 3551 cm^{-1} , a weak band 3532 cm^{-1} and a strong band 3480 cm^{-1} (Galuskina et al. 2009). On the corresponding spectra of chegemite $\text{Ca}_7(\text{SiO}_4)_3(\text{OH,F})_2$ there are a doublet 3563 and 3551 cm^{-1} , a weak band 3531 cm^{-1} and a strong band 3478 cm^{-1} (Galuskin et al. 2009). The (OH+F) content decreases with decreasing Ca/Si ratio in the sequence $\text{Ca}_5(\text{SiO}_4)_2(\text{OH,F})_2 \rightarrow \text{Ca}_7(\text{SiO}_4)_3(\text{OH,F})_2 \rightarrow \text{Ca}_9(\text{SiO}_4)_4(\text{OH,F})_2$. Thus, the intensity of OH-characteristic bands on the edgrewite and hydroxyledegrewite spectra is relatively low (Figs. 4C–4D and 5C–5D). In Raman/FTIR spectra of hydroxyledegrewite (OH > F) the band characteristic for OH-dominant Ca-humite minerals at 3475/3486 cm^{-1} does not always appear, but the band near 3550/3554 cm^{-1} is more intense than the band near 3550 cm^{-1} in edgrewite spectra compared to the intensity of main Si-O stretching bands.

In analogy to kumtyubeite the following interpretation of FTIR and Raman spectra of edgrewite and hydroxyledegrewite can be proposed considering the correlation between frequency of OH stretching vibrations and $D_{\text{O-O}}$ interatomic distance O-H \cdots O: $\nu (\text{cm}^{-1}) = 3592 - 304 \times 10^9 \times \exp(-d_{\text{O-O}}/0.1321)$ (Libowitzky

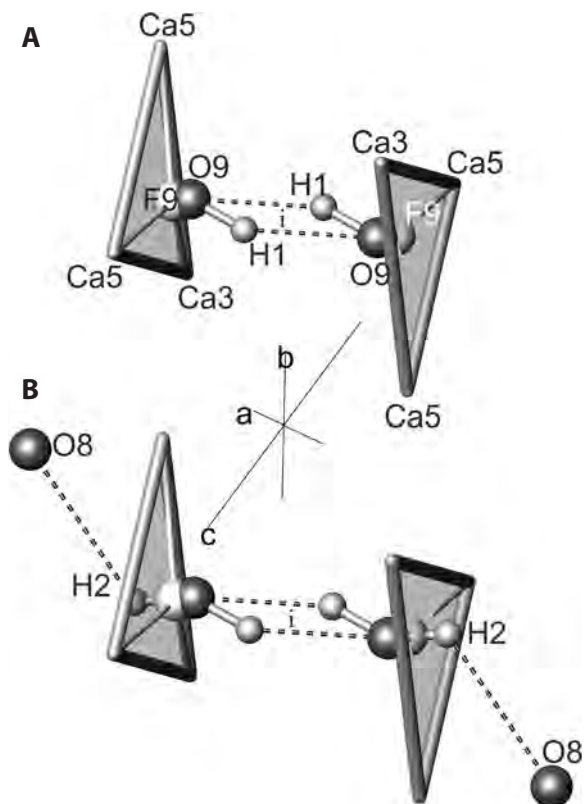


FIGURE 8. Hydrogen bonding in hydroxyledegrewite: A center of inversion (*i*) at the origin is responsible for the proximity of two adjacent H sites leading to H disorder. F9 partially replaces O9. F9 is almost in the center of the coordination triangle formed by Ca3 and 2x Ca5, whereas the larger O9 is centered outside of the plane. (A) The two H1 sites are too close for simultaneous occupation. Thus, if the occupation of F9 > O9 hydrogen bonds of the type O9-H1...F9 exist. (B) If the occupation of O9 > F9 a new type of hydrogen bond O9-H2...O8 exists.

1999). Configurations of hydrogen bonds are available from structural data. For hydroxyledegrewite the hydrogen bond O9-H1...O9 ($D_{O-O} = 2.81 \text{ \AA}$) is related to the band near $3475/3486 \text{ cm}^{-1}$ (Raman/FTIR, respectively; calculated $D_{O-O} = 2.86\text{--}2.88 \text{ \AA}$). Bands near 3555 cm^{-1} (calculated $D_{O-O} = 3 \text{ \AA}$) are due to the configurations O9-H2...O8 = 3.21 \AA (calculated frequency 3584 cm^{-1}) and O9-H1...F9 = 3.07 \AA (calculated frequency 3567 cm^{-1} for D_{O-O}). A discrepancy between calculated and experimental data are obvious in those cases where O9 is simultaneously both donor and acceptor of hydrogen bonds, e.g., O8...H2-O9...H1-O9. In this case H2-O9 should slightly shift toward O8, i.e., the hydrogen bond is reinforced and as a result the band shifts toward lower frequency. The configurations O9-H1...O9 ($D_{O-O} = 2.76 \text{ \AA}$) and O9-H2...O8 = 3.23 \AA are unlikely in edgrewite and the band near 3480 cm^{-1} is absent, in addition, the band near 3555 cm^{-1} has significantly lower intensity compared to corresponding bands on the hydroxyledegrewite spectrum.

ACKNOWLEDGMENTS

The work is partly supported by the Ministry of Science and Higher Education of Poland, grant number N307 100238. The authors thank to Igor Pekov and an anonymous reviewer for their careful revision that improved the early version of the manuscript. The authors thank E. Grew for the comments on earlier versions of the manuscript.

REFERENCES CITED

- Berry, A.J. and James, M. (2001) Refinement of hydrogen positions in synthetic hydroxyl-clinohumite by powder neutron diffraction. *American Mineralogist*, 86, 181–184.
- Bruker (1999) SMART and SAINT-Plus. Versions 6.01. Bruker AXS Inc., Madison, Wisconsin, U.S.A.
- Christie, O.H.J. (1965) Substitutions in the olivine layer of norbergite. *Norsk Geologisk Tidsskrift*, 45, 429–433.
- Czaya, R. (1971) Refinement of the structure of $\gamma\text{-Ca}_2\text{SiO}_4$. *Acta Crystallographica*, B, 27, 848–849.
- Deer, W.A., Howie, R.A., and Zussman, J. (1982) *Rock-forming Minerals, Orthosilicates*, vol. 1A, 2nd ed., 936 p. Longman, London.
- Ferraris, G., Prencipe, M., Sokolova, E.V., Gekimiyants, V.M., and Spiridonov, E.M. (2000) Hydroxylclinohumite, a new member of the humite group: Twinning, crystal structure and crystal chemistry of the clinohumite subgroup. *Zeitschrift für Kristallographie*, 215, 169–173.
- Friedrich, A., Lager, G.A., Kunz, M., Chakoumakos, B.C., Smyth, J., and Schultz, A. (2001) Temperature-dependent single-crystal neutron diffraction study of natural chondrodite and clinohumites. *American Mineralogist*, 86, 981–989.
- Frost, R.L., Palmer, S.J., and Reddy, B.J. (2007a) Near-infrared and mid-IR spectroscopy of selected humite minerals. *Vibrational Spectroscopy*, 44, 154–161.
- Frost, R.L., Palmer, S.J., Bouzaid, J.M., and Reddy, B.J. (2007b) A Raman spectroscopic study of humite minerals. *Journal of Raman Spectroscopy*, 38, 68–77.
- Galuskin, E.V., Gazeev, V.M., Armbruster, T., Zadov, A.E., Galuskina, I.O., Pertsev, N.N., Dzierzanowski, P., Kadiyski, M., Gurbanov, A.G., Wrzalik, R., and Winiarski, A. (2008) Lakargite, Ca_2ZrO_5 : a new mineral of the perovskite group from the North Caucasus, Kabardino-Balkaria, Russia. *American Mineralogist*, 93, 1903–1910.
- Galuskin, E.V., Gazeev, V.M., Lazic, B., Armbruster, T., Galuskina, I.O., Zadov, A.E., Pertsev, N.N., Wrzalik, R., Dzierzanowski, P., Gurbanov, A.G., and Bzowska, G. (2009) Chegemite, $\text{Ca}_7(\text{SiO}_4)_3(\text{OH})_2$ —a new calcium mineral of the humite-group from the Northern Caucasus, Kabardino-Balkaria, Russia. *European Journal of Mineralogy*, 21, 1045–1059.
- Galuskin, E.V., Galuskina, I.O., Dzierzanowski, P., Prusik, K., Pertsev, N.N., Zadov, A.E., Bailau, R., and Gurbanov, A.G. (2011a) Megawite, CaSnO_3 : a new perovskite-group mineral from skarns of the Upper Chegem caldera, Kabardino-Balkaria, Northern Caucasus, Russia. *Mineralogical Magazine*, 75, 2563–2572.
- Galuskin, E.V., Galuskina, I.O., Lazic, B., Armbruster, T., Zadov, A.E., Krzykavski, T., Banasik, K., Gazeev, V.M., and Pertsev, N.N. (2011b) Rusinovite $\text{Ca}_{10}(\text{Si}_2\text{O}_7)_2\text{Cl}_2$ —a new skarn mineral from the Upper Chegem caldera, Kabardino-Balkaria, Northern Caucasus, Russia. *European Journal of Mineralogy*, 23, 837–844.
- Galuskin, E.V., Armbruster, T., Galuskina, I.O., Lazic, B., Winiarski, A., Gazeev, V.M., Dzierzanowski, P., Zadov, A.E., Pertsev, N.N., Wrzalik, R., Gurbanov, A.G., and Janeczek, J. (2011c) Vorlanite $(\text{CaU}^{6+})\text{O}_8$ —a new mineral from the Upper Chegem caldera, Kabardino-Balkaria, Northern Caucasus, Russia. *American Mineralogist*, 96, 188–196.
- Galuskin, E.V., Bailau, R., Galuskina, I.O., Prusik, A.K., Gazeev, V.M., Zadov, A.E., Pertsev, N.N., Jezak, L., Gurbanov, A.G., and Dubrovinsky, L. (2011d) Eltybyuyite, IMA 2011-022. CNMNC Newsletter No. 10, October 2011, p. 2553; *Mineralogical Magazine*, 75, 2549–2561.
- Galuskin, E.V., Gfeller, F., Savelyeva, V.B., Armbruster, T., Lazic, B., Galuskina, I.O., Tobbens, D.M., Zadov, A.E., Dzierzanowski, P., Pertsev, N.N., and Gazeev, V.M. (2012) Pavlovskiyite $\text{Ca}_8(\text{SiO}_4)_2(\text{Si}_2\text{O}_7)$ —a new mineral of altered silicate-carbonate xenoliths from the two Russian type localities: Birkhin massif, Baikal Lake area and Upper Chegem caldera, North Caucasus. *American Mineralogist*, 97, 503–512, DOI: <http://dx.doi.org/10.2138/am.2012.3970>.
- Galuskina, I.O., Lazic, B., Armbruster, T., Galuskin, E.V., Gazeev, V.M., Zadov, A.E., Pertsev, N.N., Jezak, E., Wrzalik, R., and Gurbanov, A.G. (2009) Kumtyubeite $\text{Ca}_3(\text{SiO}_4)_2\text{F}_2$ —a new calcium mineral of the humite group from Northern Caucasus, Kabardino-Balkaria, Russia. *American Mineralogist*, 94, 1361–1370.
- Galuskina, I.O., Galuskin, E.V., Armbruster, T., Lazic, B., Dzierzanowski, P., Gazeev, V.M., Prusik, K., Pertsev, N.N., Winiarski, A., Zadov, A.E., Wrzalik, R., and Gurbanov, A.G. (2010a) Bitikleite-(SnAl) and bitikleite-(ZrFe)—new garnets from xenoliths of the Upper Chegem volcanic structure, Kabardino-Balkaria, Northern Caucasus, Russia. *American Mineralogist*, 95, 959–967.
- Galuskina, I.O., Galuskin, E.V., Armbruster, T., Lazic, B., Kusz, J., Dzierzanowski, P., Gazeev, V.M., Pertsev, N.N., Prusik, K., Zadov, A.E., Winiarski, A., Wrzalik, R., and Gurbanov, A.G. (2010b) Elbrusite-(Zr)—a new uranian garnet from the Upper Chegem caldera, Kabardino-Balkaria, Northern Caucasus, Russia. *American Mineralogist*, 95, 1172–1181.
- Galuskina, I.O., Galuskin, E.V., Dzierzanowski, P., Gazeev, V.M., Prusik, K., Pertsev, N.N., Winiarski, A., Zadov, A.E., and Wrzalik, R. (2010c) Toturite $\text{Ca}_3\text{Sn}_2\text{Fe}_2\text{SiO}_{12}$ —a new mineral species of the garnet group. *American Mineralogist*, 95, 1305–1311.

- Galuskina, I.O., Galuskin, E.V., Kusz, J., Dzierzanowski, P., Prusik, K., Gazeev, V.M., Pertsev, N.N., and Dubrovinsky, L. (2011a) Bitikleite-(SnFe), IMA 2010-064. CNMNC Newsletter, April 2011, p. 290; Mineralogical Magazine, 75, 289–294.
- Galuskina, I.O., Galuskin, E.V., Prusik, K., Gazeev, V.M., Pertsev, N.N., and Dzierzanowski, P. (2011b) Irinarassite, IMA 2010-073. CNMNC Newsletter No. 8, April 2011, p. 292; Mineralogical Magazine, 75, 289–294.
- Galuskina, I.O., Lazic, B., Galuskin, E.V., Armbruster, T., Gazeev, V.M., Wlodyka, R., Zadov, A.E., Dulski, M., and Dzierzanowski, P. (2012) Fluorhegemite, IMA2011-112. CNMNC Newsletter No. 13, June 2012, p. 812, Mineralogical Magazine, 76, 807–817.
- Gazeev, V.M., Zadov, A.E., Gurbanov, A.G., Pertsev, N.N., Mokhov, A.V., and Dokuchaev, A.Y. (2006) Rare minerals from Verkhniechegemskaya caldera (in xenoliths of skarned limestone). Vestnik Vladikavkazskogo Nauchnogo Centra, 6, 18–27 (in Russian).
- Gibbs, G.V. and Ribbe, P.H. (1969) The crystal structure of the humite minerals: I. Norbergite. American Mineralogist, 54, 376–390.
- Gobechiya, E.R., Yamnova, N.A., Zadov, A.E., and Gazeev, V.M. (2008) Calcio-olivine γ -Ca₂SiO₄: I. Rietveld refinement of the crystal structure. Crystallography Report, 53, 404–408.
- Grew, E.S., Locock, A.J., Mills, S.J., Galuskina, I.O., Galuskin, E.V., and Halenius U. (2012) Counting Garnets: A New Nomenclature of the Garnet Supergroup. In Abstracts of European Mineralogical Conference, Vol. 1, EMC2012-21-2, Frankfurt/Main, Germany.
- Jones, N.W. (1969) Crystallographic nomenclature and twinning in the humite minerals. American Mineralogist, 54, 309–313.
- Kirfel, A., Hamm, H.M., and Will, G. (1983) The crystal structure of reinhardbraunsite, Ca₃(SiO₄)₂(OH,F)₂, a new mineral of the calcio-chondrodite type. Tschermarks Mineralogische und Petrographische Mitteilungen, 31, 137–150.
- Kraus, W. and Nolze, G. (1996) POWDER CELL—a program for the representation and manipulation of crystal structures and calculation of resulting X-ray powder patterns. Journal of Applied Crystallography, 29, 301–303.
- Lazic, B., Armbruster, T., Savelyeva, V.B., Zadov, A.E., Pertsev, N.N., and Dzierzanowski, P. (2011) Galuskinite, Ca₇(SiO₄)₃(CO₃), a new skarn mineral from the Birkhin gabbro massif, Eastern Siberia, Russia. Mineralogical Magazine, 75, 2631–2548.
- Libowitzky, E. (1999) Correlation of O-H stretching frequencies and O-H-O hydrogen bond lengths in minerals. Monatshefte für Chemie, 130, 1047–1059.
- Mumme, W.G., Hill, R.J., Bushnell-Wye, G., and Segnit, E.R. (1995) Rietveld crystal structure refinements, crystal chemistry and calculated powder diffraction data for the polymorphs of dicalciumsilicate and related phases. Neues Jahrbuch für Mineralogie Abhandlungen, 169, 35–68.
- Ribbe, P.H. (1982) The humite series and Mn-analogs. In P.H. Ribbe, Ed., Orthosilicates, 5, 231–274. Reviews of Mineralogy, Mineralogical Society of America, Chantilly, Virginia.
- Robinson, K., Gibbs, G.V., and Ribbe, P.H. (1973) The crystal structures of the humite minerals. IV. Clinohumite and titanoclinohumite. American Mineralogist, 58, 43–49.
- Shannon, R.D. (1976) Revised effective ionic radii and systematic studies of interatomic distances in halides and chalcogenides. Acta Crystallographica, A, 31, 751–767.
- Sheldrick, G.M. (1996) SADABS. University of Göttingen, Germany.
- (2008) A short history of SHELX. Acta Crystallographica A, 64, 112–122.
- Smith, D.N., Majumdar, A., and Ordway, F. (1965) The crystal structure of γ -dicalcium silicate. Acta Crystallographica, 18, 787–795.
- Taylor, W.H. and West, J. (1928) The crystal structure of the chondrodite series. Proceedings of the Royal Society (London), A, 117, 517–532.
- Thompson, J.B. (1978) Biopyriboles and polysomatic series. American Mineralogist, 63, 239–249.
- Udagawa, S., Urabe, K., Natsume, M., and Yano, T. (1980) Refinement of the crystal structure of γ -Ca₂SiO₄. Cement and Concrete Research, 10, 239–144.
- Yamnova, N.A., Zubkova, N.V., Eremin, N.N., Zadov, A.E., and Gazeev, V.M. (2011) Crystal structure of larnite β -Ca₂SiO₄ and specific features of polymorphic transitions in dicalcium orthosilicate. Crystallography Reports, 56, 210–220.
- Zadov, A.E., Gazeev, V.M., Pertsev, N.N., Gurbanov, A.G., Yamnova, N.A., Gobechiya, E.R., and Chukanov, N.V. (2008) Discovery and investigation of a natural analog of calcio-olivine (γ -Ca₂SiO₄). Doklady Earth Sciences, 423A, 1431–1434 (in Russian).
- Zadov, A.E., Gazeev, V.M., Karimova, O.V., Pertsev, N.N., Pekov, I.V., Galuskin, E.V., Galuskina, I.O., Gurbanov, A.G., Belakovskiy, D.I., Borisovskiy, S.E., and others. (2011a) Magnesioheptite KNa₂Li(Mg,Fe)₂Ti₃Si₈O₂₄—A new mineral of the neptunite group. Zapiski RMO, 1, 57–66 (in Russian).
- Zadov, A.E., Pekov, I.V., Gazeev, V.M., Zubkova, N.V., Yapaskurt, V.O., Chukanov, N.V., Kartashov, P.M., Galuskin, E.V., Galuskina, I.O., Pertsev, N.N., and others. (2011b) Aklimaite, IMA 2011-050. CNMNC Newsletter No. 10, October 2011, p. 2560; Mineralogical Magazine, 75, 2549–2561.
- Zenser, L.-P., Gruehn, R., and Weil, M. (2000) Synthese, Charakterisierung und Struktur von Mn₃SiO₄F₂. Zeitschrift für Anorganische und Allgemeine Chemie, 626, 871–877.
- Zharikov, V.A., Rusinov, V.L., Marakushev, A.A., Zaraysky, G.P., Omel'yanchenko, B.I., Pertsev, N.N., Rass, I.T., Andreeva, O.V., Abramov, C.C., and Podlesski, K.V. (1998) Metasomatism and metasomatic rocks. Nauka Publication, Moscow, 489 p. (in Russian).

MANUSCRIPT RECEIVED MARCH 7, 2012

MANUSCRIPT ACCEPTED JULY 26, 2012

MANUSCRIPT HANDLED BY ANDREW McDONALD

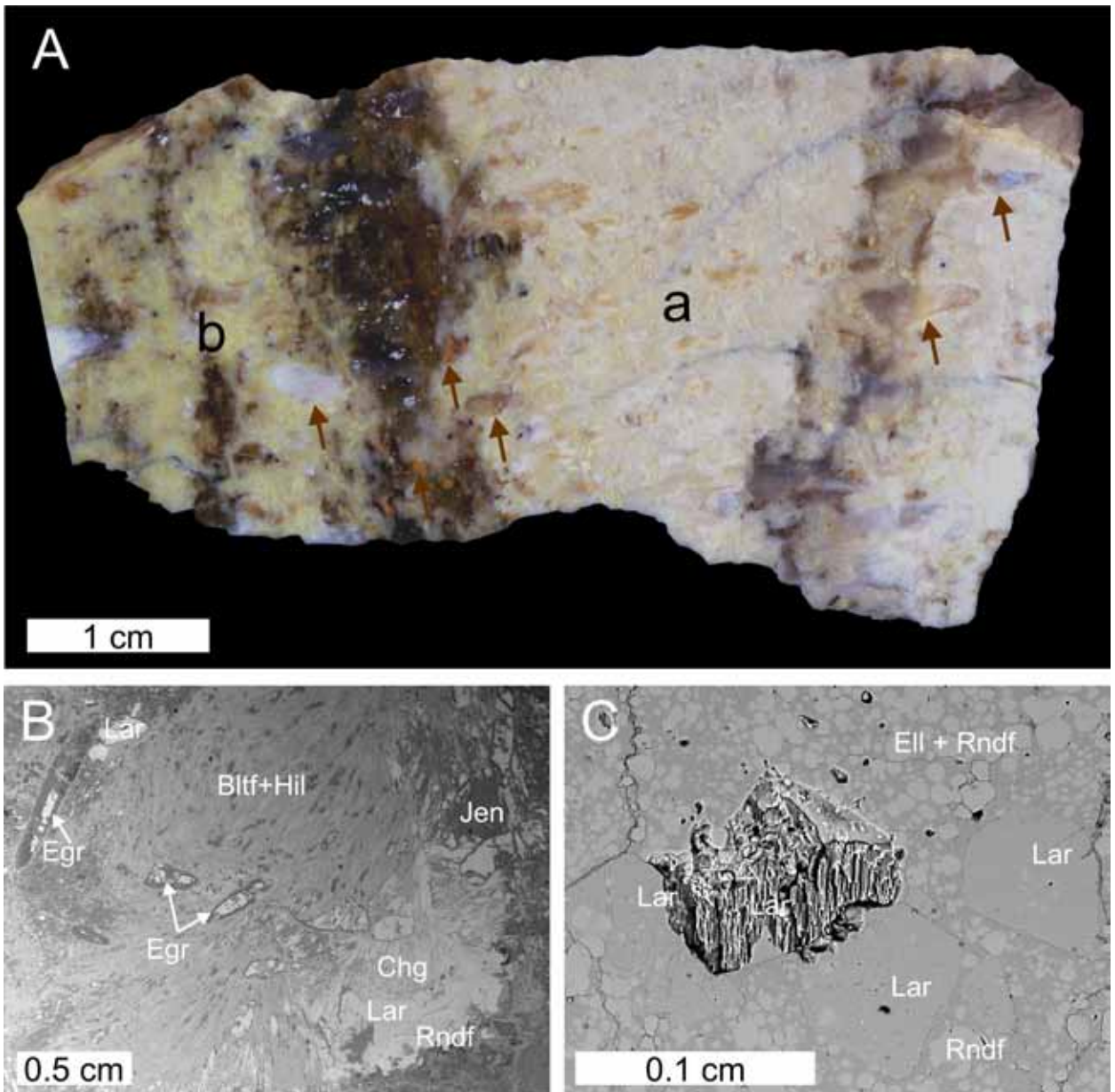


FIGURE 1. (supplementary materials). A. Altered lamite skarn comprising a cream-colored zone (a) containing edgrewite (Fig. 1B) and a yellowish zone (b) commonly stained brown-dark by iron hydroxides and sulfates. Arrows point to lenticular aggregates with lamite relics (e.g., Fig. 1C) and to yellow and light-brown “hydrogarnet” pseudomorphs with shapes resembling mafic phenocrysts (pyroxene, amphibole, biotite) in ignimbrite. (b) Backscattered electron image of an area in the cream-colored zone showing altered skarn with lamite and rondorfite relics and characteristic atoll-like microstructure with edgrewite. (c) Backscattered electron image of a primary skarn relic with lamite and rondorfite crystals in hydroxyllellestadite. Bltf = bultfonteinite, Chg = chegemite-fluorchegemite, Egr = edgrewite, Ell = hydroxyllellestadite, = jennite, Lar = lamite, Hil = hillebrandite, Rndf = rondorfite, Trb = trabzonite.

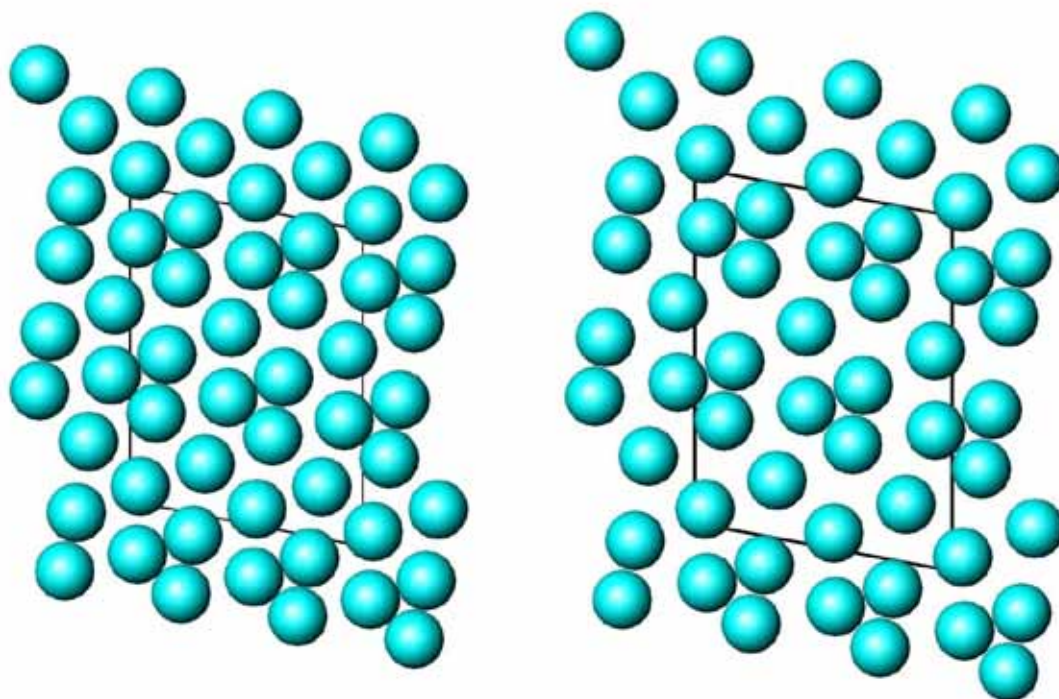


FIGURE 7. (supplementary materials). Left: Anion arrangement in clinohumite $\text{Mg}_9(\text{SiO}_4)_4(\text{F},\text{OH})_2$ viewed along the short **a** axis ($P2_1/c11$ setting); each oxygen is represented as a sphere of 1.3 Å radius. Right: corresponding anion arrangement in the structure of edgrewite $\text{Ca}_9(\text{SiO}_4)_4(\text{F},\text{OH})_2$. The large Ca at octahedral sites stretches the close-packed anion arrangement.

Table 2. (supplementary materials) Calculated powder diffraction pattern of edgrewite ($\text{CuK}\alpha_{1+2} = 1.540598$, 1.544426; geometry: Debye-Scherrer, fixed slit, no anomalous dispersion; condition: $I > 4$)

<i>h</i>	<i>k</i>	<i>l</i>	2Theta	d_{hkl}	I_{rel}	<i>h</i>	<i>k</i>	<i>l</i>	2Theta	d_{hkl}	I_{rel}
0	0	1	5.834	15.1377	4	2	1	2	38.755	2.3217	7
0	2	-1	15.866	5.5811	21	1	1	-7	44.878	2.0181	9
0	2	1	17.905	4.9501	5	1	5	1	45.759	1.9813	6
0	2	-2	17.912	4.9482	11	2	2	4	47.652	1.9069	53
1	0	2	21.078	4.2116	16	2	2	-5	47.661	1.9065	54
0	2	2	21.430	4.1432	18	1	1	7	47.744	1.9034	5
0	2	-3	21.440	4.1413	14	2	4	-1	48.083	1.8908	36
1	1	2	23.306	3.8137	42	2	4	1	49.655	1.8345	11
0	0	4	23.489	3.7844	8	2	4	-3	49.663	1.8343	7
1	2	0	23.691	3.7525	10	0	6	1	50.465	1.8070	12
1	2	-1	23.693	3.7522	5	0	6	-4	50.479	1.8065	12
1	1	-3	25.119	3.5424	33	1	3	6	50.566	1.8036	14
1	2	-3	27.796	3.2070	4	1	5	3	50.919	1.7919	10
1	1	-4	29.336	3.0420	28	1	5	-6	52.640	1.7373	8
1	3	-1	29.461	3.0294	100	0	4	6	53.185	1.7208	9
0	0	5	29.480	3.0275	11	0	4	-8	53.211	1.7200	8
1	3	0	29.759	2.9997	24	1	3	-8	53.226	1.7196	9
0	2	4	30.864	2.8949	16	2	4	-5	54.191	1.6912	5
0	2	-5	30.877	2.8937	14	0	0	9	54.513	1.6820	34
1	3	1	31.219	2.8627	29	3	1	0	54.917	1.6705	6
0	4	-1	31.481	2.8395	7	0	6	3	55.658	1.6501	21
1	1	4	31.669	2.8231	79	0	6	-6	55.682	1.6494	21
1	3	-3	32.354	2.7648	65	3	1	2	56.710	1.6219	7
0	4	1	33.680	2.6590	11	1	7	-2	59.820	1.5448	19
0	4	-3	33.691	2.6581	9	3	3	-1	59.923	1.5424	5
1	3	2	33.705	2.6570	31	3	1	4	61.212	1.5130	5
1	1	-5	34.133	2.6247	55	3	3	-3	61.626	1.5038	5
2	0	0	35.389	2.5344	11	1	3	8	61.661	1.5030	6
1	2	4	35.689	2.5138	17	3	1	-5	62.729	1.4800	4
1	2	-5	35.700	2.5130	18	3	2	4	63.725	1.4592	7
1	4	-1	36.233	2.4773	24	3	2	-5	63.733	1.4591	7
2	1	0	36.321	2.4715	12	3	4	-1	64.081	1.4520	4
1	1	5	36.688	2.4476	5	1	3	-10	64.677	1.4400	5
1	3	3	37.036	2.4254	8						

Table 3. (supplementary materials) Calculated powder diffraction pattern of hydroxyldegrewite ($\text{CuK}\alpha_{1+2} = 1.540598, 1.544426$; geometry: Debye-Scherrer, fixed slit, no anomalous dispersion; condition: $I > 4$)

<i>h</i>	<i>k</i>	<i>l</i>	2Theta	d_{hkl}	I_{rel}	<i>h</i>	<i>k</i>	<i>l</i>	2Theta	d_{hkl}	I_{rel}
0	0	1	5.836	15.1320	4	0	4	-5	39.677	2.2698	4
0	2	-1	15.872	5.5792	20	2	1	-3	39.941	2.2554	4
0	2	1	17.909	4.9490	4	1	1	-7	44.897	2.0173	9
0	2	-2	17.919	4.9461	10	1	5	1	45.771	1.9808	6
1	0	2	21.084	4.2102	16	2	2	4	47.667	1.9063	52
0	2	2	21.434	4.1422	18	2	2	-5	47.680	1.9058	53
0	2	-3	21.449	4.1394	14	1	1	7	47.760	1.9028	5
1	1	2	23.312	3.8126	41	1	3	-7	48.063	1.8915	4
0	0	4	23.498	3.7830	7	2	4	-1	48.099	1.8902	35
1	2	0	23.698	3.7515	9	2	4	1	49.670	1.8340	11
1	2	-1	23.701	3.7510	5	2	4	-3	49.681	1.8336	7
1	1	-3	25.129	3.5410	32	0	6	1	50.478	1.8066	12
1	2	1	25.132	3.5405	3	0	6	-4	50.499	1.8059	12
1	2	-3	27.807	3.2057	4	1	3	6	50.580	1.8031	14
1	1	-4	29.348	3.0409	27	1	5	3	50.931	1.7915	10
1	3	-1	29.471	3.0285	100	1	5	-6	52.663	1.7366	8
0	0	5	29.491	3.0264	11	0	4	6	53.199	1.7204	9
1	3	0	29.768	2.9989	24	0	4	-8	53.237	1.7192	7
0	2	4	30.872	2.8941	16	1	3	-8	53.250	1.7188	8
0	2	-5	30.891	2.8924	14	2	4	-5	54.213	1.6906	5
1	3	1	31.227	2.8620	28	0	0	9	54.535	1.6813	33
0	4	-1	31.491	2.8386	7	3	1	0	54.935	1.6701	5
1	1	4	31.679	2.8222	78	0	6	3	55.672	1.6497	20
1	3	-3	32.367	2.7638	65	0	6	-6	55.707	1.6487	21
0	4	1	33.688	2.6583	11	3	1	2	56.728	1.6214	6
0	4	-3	33.704	2.6571	9	1	3	-9	58.804	1.5690	4
1	3	2	33.714	2.6564	31	1	7	-2	59.841	1.5443	18
1	1	-5	34.147	2.6236	55	3	3	-1	59.943	1.5419	5
2	0	0	35.400	2.5336	11	3	1	4	61.232	1.5125	5
1	2	4	35.699	2.5131	17	3	3	-3	61.648	1.5033	5
1	2	-5	35.715	2.5120	17	1	3	8	61.681	1.5026	6
1	4	-1	36.244	2.4765	24	3	1	-5	62.751	1.4795	4
2	1	0	36.332	2.4707	12	3	2	4	63.746	1.4588	7
1	1	5	36.700	2.4468	5	3	2	-5	63.757	1.4586	6
1	3	3	37.045	2.4248	8	3	4	-1	64.103	1.4515	4
2	1	2	38.766	2.3210	7	1	3	-10	64.708	1.4394	5

Table 5. (supplementary materials) Comparison of optical properties of Ca-humites

	Kumtyubeite	Chegemite	Chegemite	Edgrewite	Hydroxyledgrewite
	xenolith 1	xenolith 1	xenolith 7	xenolith 1	xenolith 1
X _c	15(2)°	0°	0°	12(2)°	12(2)°
Sign	-	-	-	+	+
2V	40-55°	72-88°	76-86	75-85°	75-85°
α	1.594(2)	1.621(2)	1.630(2)	1.621(2)	1.625(2)
β	1.605(2)	1.626(3)	1.636(2)	1.625(2)	1.629(2)
γ	1.608(2)	1.630(2)	1.640(2)	1.631(2)	1.635(2)
Δ	0.014	0.009	0.010	0.010	0.010

Table 6. (supplementary materials) Comparison of chemical compositions of Ca-humites

wt%	Kumtyubeite	Chegemite	Edgrewite
SiO ₂	28.44	30.00	30.95
TiO ₂	0.06	0.02	0.09
CaO	66.58	65.49	65.23
F	4.84	3.57	2.83
H ₂ O*	1.98	1.32	0.99
	101.90	100.39	100.09
O=F+Cl	2.04	1.50	1.19
	99.86	98.89	98.89
Ca	5.003	7.004	9.004
Si	1.994	2.994	3.987
Ti ⁴⁺	0.003	0.001	0.009
OH	0.926	0.876	0.846
F	1.074	1.126	1.154
Ca/Si	~2.5	~2.33	~2.25

formula calculated on 18(O+F+OH), * - calculated on charge balance

Table 8a. (supplementary materials) Anisotropic atomic displacement parameters (\AA^2) for edgrewite.

Atom	U_{11}	U_{22}	U_{33}	U_{23}	U_{13}	U_{12}
Ca1	0.0044(2)	0.0098(3)	0.0075(3)	0.0039(2)	-0.0010(2)	0.0002(2)
Ca2	0.00458(18)	0.0082(2)	0.00785(19)	0.00066(15)	0.00088(13)	0.00077(13)
Ca3	0.00553(18)	0.00596(19)	0.00842(19)	0.00282(15)	-0.00017(14)	0.00040(14)
Ca4	0.00513(18)	0.00561(19)	0.00779(19)	0.00211(14)	-0.00006(14)	-0.00014(14)
Ca5	0.00614(19)	0.0075(2)	0.00770(18)	0.00270(14)	-0.00082(14)	0.00003(14)
Si1	0.0017(2)	0.0053(3)	0.0064(2)	0.0024(2)	-0.00003(18)	-0.00007(18)
Si2	0.0023(2)	0.0052(3)	0.0070(3)	0.0026(2)	0.00012(19)	0.00021(18)
O1	0.0032(6)	0.0092(7)	0.0101(7)	0.0027(6)	-0.0005(5)	-0.0002(5)
O2	0.0054(6)	0.0047(7)	0.0092(7)	0.0035(5)	0.0004(5)	-0.0003(5)
O3	0.0059(7)	0.0082(7)	0.0078(7)	0.0038(5)	0.0004(5)	-0.0007(5)
O4	0.0054(6)	0.0090(7)	0.0077(6)	0.0016(6)	0.0001(5)	0.0002(5)
O5	0.0044(7)	0.0077(7)	0.0113(7)	0.0041(6)	-0.0001(5)	0.0000(5)
O6	0.0071(7)	0.0041(7)	0.0100(7)	0.0031(5)	0.0011(5)	0.0002(5)
O7	0.0061(6)	0.0078(7)	0.0087(7)	0.0033(5)	-0.0002(5)	0.0007(5)
O8	0.0059(6)	0.0079(7)	0.0065(6)	0.0023(5)	-0.0002(5)	0.0001(5)

Note: The anisotropic atomic displacement factor exponent takes the form: $-2\pi^2 [h^2 \mathbf{a}^{*2} U_{11} + \dots + 2hk \mathbf{a}^* \mathbf{b}^* U_{12}]$

Table 8b. (supplementary materials) Anisotropic atomic displacement parameters (\AA^2) for hydroxyledgrewite.

Atom	U_{11}	U_{22}	U_{33}	U_{23}	U_{13}	U_{12}
Ca1	0.00786(15)	0.01119(14)	0.00793(14)	0.00293(11)	-0.00111(10)	0.00046(10)
Ca2	0.00786(11)	0.01000(11)	0.00823(11)	-0.00042(8)	0.00119(7)	0.00077(7)
Ca3	0.00902(11)	0.00734(10)	0.00887(11)	0.00193(8)	-0.00022(7)	0.00047(7)
Ca4	0.00870(11)	0.00686(10)	0.00835(11)	0.00133(8)	-0.00018(7)	-0.00025(7)
Ca5	0.00966(11)	0.00912(11)	0.00793(10)	0.00165(8)	-0.00081(7)	0.00025(7)
Si1	0.00570(14)	0.00672(13)	0.00670(13)	0.00109(10)	-0.00008(10)	0.00009(10)
Si2	0.00596(14)	0.00678(13)	0.00712(13)	0.00099(10)	0.00019(10)	0.00000(10)
O1	0.0063(4)	0.0113(3)	0.0104(3)	0.0021(3)	-0.0003(3)	0.0003(3)
O2	0.0083(4)	0.0068(3)	0.0097(3)	0.0016(3)	0.0000(3)	-0.0002(3)
O3	0.0087(4)	0.0100(3)	0.0083(3)	0.0030(3)	0.0002(3)	-0.0005(3)
O4	0.0089(4)	0.0092(3)	0.0089(3)	0.0003(3)	-0.0002(3)	-0.0005(3)
O5	0.0068(3)	0.0104(3)	0.0117(3)	0.0019(3)	-0.0005(3)	0.0000(3)
O6	0.0097(4)	0.0070(3)	0.0105(3)	0.0014(3)	0.0003(3)	0.0001(3)
O7	0.0093(4)	0.0099(3)	0.0083(3)	0.0024(3)	0.0000(3)	0.0006(3)
O8	0.0087(4)	0.0091(3)	0.0086(3)	-0.0002(3)	0.0001(3)	0.0001(3)

Note: The anisotropic atomic displacement factor exponent takes the form: $-2\pi^2 [h^2 \mathbf{a}^{*2} U_{11} + \dots + 2hk \mathbf{a}^* \mathbf{b}^* U_{12}]$

Table 9. (supplementary materials)
Bond lengths (Å) for edgrewite and
hydroxyledgrewite

Atom1	Atom2	Bond lengths	Bond lengths
		F-dominant	OH-dominant
Ca1	O2	2.3106(14) (2x)	2.3096(7) (2x)
	O1	2.3734(15) (2x)	2.3727(7) (2x)
	O4	2.3955(15) (2x)	2.3957(7) (2x)
	Mean	2.360	2.359
Ca2	O6	2.3078(16)	2.3064(8)
	O2	2.3287(15)	2.3292(8)
	O5	2.3759(15)	2.3754(8)
	O3	2.3794(15)	2.3824(8)
	O1	2.3970(15)	2.3951(8)
	O7	2.3989(15)	2.4015(8)
	Mean	2.365	2.365
Ca3	F9	2.278 (4)	2.281(2)
	O3	2.3087(16)	2.3077(8)
	O6	2.3222(15)	2.3203(7)
	O9	2.365(5)	2.345(2)
	O7	2.4126(15)	2.4123(8)
	O8	2.4417(16)	2.4382(8)
	O5	2.4685(16)	2.4678(8)
	Mean ¹	2.386	2.382
	Mean ²	2.371	2.371
Ca4	O2	2.3146(15)	2.3105(7)
	O4	2.3557(15)	2.3557(8)
	O7	2.3727(16)	2.3686(7)
	O3	2.4306(15)	2.4282(8)
	O4	2.4596(16)	2.4588(8)
	O1	2.4635(15)	2.4611(8)
	Mean	2.399	2.397
Ca5	F9	2.272(4)	2.262(3)
	O8	2.2783(15)	2.2788(8)
	O9	2.299(4)	2.3036(19)
	F9	2.321(4)	2.312(2)
	O9	2.332(5)	2.329(2)
	O8	2.3641(16)	2.3646(8)
	O5	2.4061(16)	2.4072(8)
	O6	2.4396(15)	2.4404(8)
	Mean ¹	2.353	2.354
	Mean ²	2.347	2.344
Si1	O1	1.6230(15)	1.6239(8)
	O3	1.6440(16)	1.6431(8)
	O4	1.6446(15)	1.6434(8)
	O2	1.6482(15)	1.6520(7)
	Mean	1.640	1.641
Si2	O5	1.6250(15)	1.6230(8)
	O6	1.6442(16)	1.6458(8)
	O7	1.6458(17)	1.6460(8)
	O8	1.6462(15)	1.6456(8)
	Mean	1.640	1.640
F9	Ca5	2.272(4)	2.262(3)
	Ca3	2.278(4)	2.281(2)
	Ca5	2.321(4)	2.312(2)
	Mean	2.290	2.285

¹considering O9 but not F9;

²considering F9 but not O9.

Table 10. (supplementary materials)
Tetrahedral angles (°) for edgrewite and
hydroxyledgrewite

O	T	O	F-dominant	OH-dominant
O3	Si1	O1	113.60(8)	113.56(4)
O4	Si1	O1	114.79(8)	114.79(4)
O4	Si1	O3	105.38(8)	105.28(4)
O2	Si1	O1	112.83(8)	112.80(4)
O2	Si1	O3	104.25(8)	104.43(4)
O2	Si1	O4	105.00(8)	105.00(4)
O6	Si2	O5	113.52(8)	113.48(4)
O7	Si2	O5	114.39(8)	114.33(4)
O7	Si2	O6	105.38(8)	105.48(4)
O8	Si2	O5	112.88(8)	112.92(4)
O8	Si2	O6	104.30(8)	104.36(4)
O8	Si2	O7	105.45(8)	105.35(4)